

Contemporary Engineering Sciences, Vol. 8, 2015, no. 16, 729-736
HIKARI Ltd, www.m-hikari.com
<http://dx.doi.org/10.12988/ces2015.53196>

Forward Modeling of SIMA Seismic Line

Fadila Ouraini

Team of modelling in fluid mechanics and environment, LPT, URAC 13
Faculty of sciences, Mohammed V University, B.P. 1014, Rabat, Morocco

Ramon Carbonell, David Marti Linares

Institute of Earth Sciences, 'Jaume Almera', CSIC
C/ Lluís Solé I Sabaris s/n 08028, Barcelona, Spain

Puy Ayarza

Geology Department, University of Salamanca
37008 Salamanca, Spain

Kamal Gueraoui*

Team of modelling in fluid mechanics and environment, LPT, URAC 13
Faculty of sciences, Mohammed V University, B.P. 1014, Rabat, Morocco

&

Department of Mechanical Engineering
University of Ottawa, Ottawa, Canada

*Corresponding author

Mimoune Harnafi

Scientific Institute of Rabat, Av. Ibn Battouta
B. P. 703, Agdal, Rabat, Morocco

Copyright © 2015 Kamal Gueraoui et al. This article is distributed under the Creative Commons Attribution License, which permits unrestricted use, distribution, and reproduction in any medium, provided the original work is properly cited.

Abstract

In this paper, a reviewed velocity model is proposed along the North-South high-resolution profile SIMA (Seismic Imaging of the Moroccan Atlas), acquired in 2010 and crossing the four major geological zones in Morocco, the High Atlas, the Middle Atlas, the western edge of the Rif Mountains and the Sahara craton. The

tremendous changes in topography of the studied area and the complex near surface layer led us to better focus on the shallow subsurface zone, and establish a revised 550 km long P-wave velocity model, based on forward modeling.

Keywords: Seismic modeling, Atlas Mountains, P-wave velocity model, traveltime tomography

Introduction

The development of seismic wave methods was led by oil and gas exploration industry, but these methodologies were quickly adopted in other exploration applications such as mineral, water, geothermal energy or waste disposal sites. These methods provide detailed information about the internal structure, the physical properties or the composition of the subsurface and also give insights about the geological evolution and the geodynamics of the target area.

We propose, through this work, a new solution, better focusing on the shallowest part, of the seismic study based on a North-South high-resolution wide-angle seismic reflection and refraction profile, crossing one of the most challenging orogens, the Moroccan Atlas mountain chains, that was carried out to image the crustal structure and the Moho geometry beneath these mountain chains obtaining a 2D, P-wave seismic velocity model [1], [2].

The interpretation of crustal seismic refraction and reflection data is carried out using a trial-and-error forward modeling approach based on two-dimensional ray tracing (e.g., [3]). The theoretical traveltime and amplitude response of a laterally inhomogeneous medium are repeatedly compared with observed record sections until a model is constructed which provides a satisfactory match between calculation and observation.

Data acquisition and processing

A controlled source seismic acquisition experiment consists on an array of sensors (geophones) usually deployed at the surface that record the seismic energy generated by an artificial source (for instance, explosives, Vibroseis trucks, accelerated weight drop or sledge hammer). Every geophone records, during a listening time window that depends on the target depth of the study, the reflected and refracted waves. These are generated by the changes of impedance in the subsurface. The movement of the ground is sampled, digitized and stored on magnetic media. The recorded seismic traces are gathered by shot point and sorted by offset (distance between receiver and shot point) to make up the data set in a seismic survey.

Seismic waves are a perturbation of the environment that propagates in space and time. The propagation depends on the elastic properties and the density of the medium and it can be described by Hooke's law, which relates the stress to de-

formation, and the second Newton's law that relates the force to the acceleration. Different kind of seismic waves are recorded in a seismic experiment, such as body waves (P- and S-wave), surface waves, Airy waves or guided waves.

Database acquisition

934 Reftek 125a (TEXANS) digital seismic recording instruments from the IRIS (Incorporated Research Institutions for Seismology)-PASSCAL Instrument Pool were deployed along the transect of almost 700 km [1]. A total of six shot points were distributed along the profile. Every shot point was charged with a 1000 kg of explosives in variable depth shot holes (30-60 m). The shot points were carefully chosen based on the field investigations. The seismic data was recorded in SEG Y format (conventional seismic format for reflection and refraction surveys). SEG Y data begins with 3200-bytes ascii header providing a human-readable description of the seismic data followed by a 400-bytes Binary File Header that contains binary values that affect the whole SEG Y file. Certain values in this header are crucial for the processing of the data in the file, particularly the sampling interval, trace length and format code. After that a 240-bytes trace header containing the attributes of the seismic trace and after this header, the amplitudes values for every sample are included for every trace. One of the main values is the coordinates of every receiver (seismic trace) and the shot point locations, which were obtained by handheld GPS [2].

Data processing

The raw seismic data set need some previous processing to enable a precise picking of the different traveltimes. First, the noisy traces are removed, and then a spherical divergence and offset amplitude recovery are applied to account for the loss of energy depending on the distance, after that the traces have been balanced [4]. The analysis of the frequency content of the data by means of frequency filters is the key factor to improve the S/N ratio. Several frequency filters were tested to determine which frequency range was richer in seismic signal energy. Similar data has been processed in the same way [4]. The butterworth band-pass filter applied to the shot gather $f = 0.25-2-6-8$ Hz basically retains all the original frequencies present in the data. The resulting processed shot gathers clearly imaged the first arrivals and even other seismic phases corresponding to intra-crustal and Moho reflections and refractions, allowing the picking up to large offsets. For imaging purposes, amplitude balance functions were applied and other gain corrections were also tested to assure a more homogeneous distribution of the energy of adjacent seismic traces to make easier the picking. Offset information was obtained from the source and receiver locations (x, y, z coordinates).

Method

The interpretation of seismic refraction and reflection data is carried out using a trial and-error forward-modeling approach based on two-dimensional ray tracing algorithm [5]. The calculated traveltimes and amplitudes responses of a laterally inhomogeneous medium are repeatedly compared with the real record sections obtained by picking, until a velocity model is constructed providing a satisfactory match between calculation and observation.

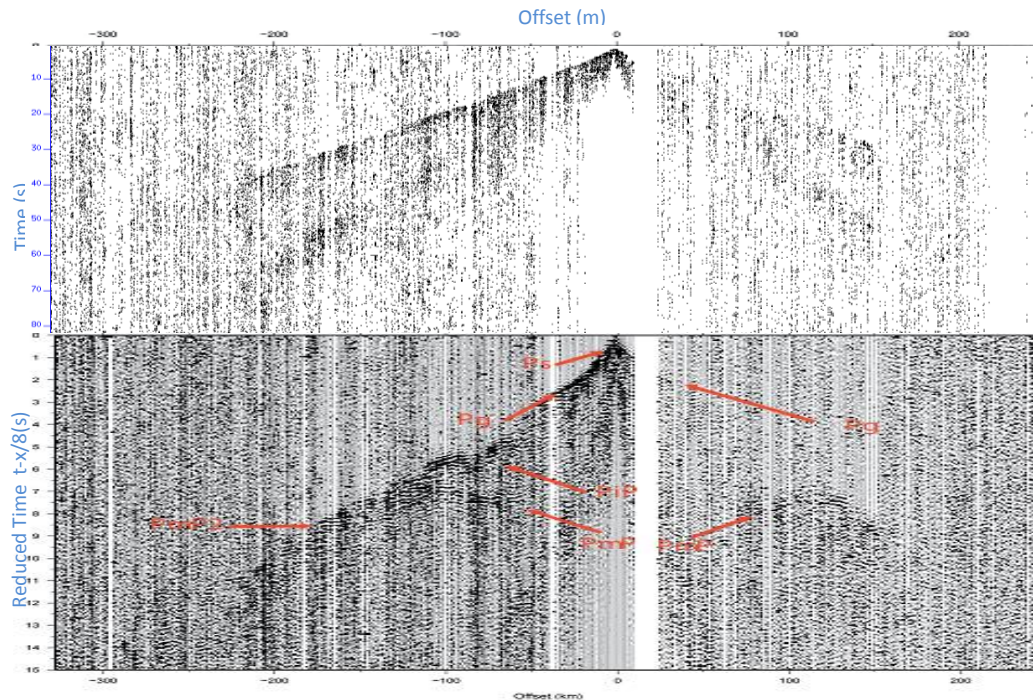


Figure 1: Record section of shot 1, before and after applying all data processing and reduction velocity, $V_{red}=8\text{km/s}$, and phase designation [1].

Traveltimes picking:

The picking of first arrivals and the imaging of the shot gathers were carried out using academic software: Seismic Unix, developed at Colorado School of Mines, GMT (Generic Mapping Tools) and other Linux open source utilities.

-First, to show the wave propagating at a certain velocity as a horizontal

hodochrone, instead of plotting the seismic traces as a function of distance or offset and time: $s(x,t)$, they are plotted as $s(x,t-x/V_{red})$, with V_{red} the reduction velocity (wanted velocity).

-Traveltime picking is based on the correlation of seismic phases with the offset on shot gathers. Shot gathers allow the identification of different phases, following the standard nomenclature for this type of dataset, these are Ps (S wave arrival), Pg

(direct arrival), PiP (reflected phase in the crust), PmP (Moho reflection) and Pn (head wave travelling within the upper mantle) ...

The cross correlation function [6] between the offset and time series of length N at a delay d used is

$$C(d) = c \sum_{n=0}^{N-1} y_1(n)y_2(n+d) \quad (1)$$

$$\text{where } 1 - N \leq d \leq N - 1; c = \left[\sum_{n=0}^{N-1} y_1^2(n) \sum_{n=0}^{N-1} y_2^2(n) \right]^{-1/2} \text{ and } y_2(i) \\ = 0 \begin{cases} i < 0 \\ i > N - 1 \end{cases}$$

Velocity model parameterization:

The initial velocity model of the routine presented can be described as a layered, 2-D isotropic P wave velocity model. Layer boundaries and upper and lower layer velocities are specified by an arbitrary number and spacing of boundary and velocity nodes [7]. The layer boundaries and velocity field within layers are determined by linear interpolation between the specified nodes, allowing both horizontal and vertical velocity gradients and velocity discontinuities across layer boundaries. Each layer is divided laterally into trapezoidal blocks separated by vertical boundaries that are included automatically wherever there is an upper or lower layer boundary node or velocity point.

For a model trapezoid (Fig. 2) that has four boundaries in the x - z plane defined by

$$x = x_1, \quad x = x_2, \quad z = s_1x + b_1, \quad z = s_2x + b_2,$$

and four corner velocities v_1 , v_2 , v_3 , and v_4 , the P-wave velocity, v , within the trapezoid is

$$v(x, z) = \frac{(c_1x + c_2x^2 + c_4xz + c_5)}{(c_6x + c_7)} \quad (2)$$

where the coefficients, c_i , are linear combinations of the corner velocities;

$$\begin{aligned} c_1 &= s_2(x_2v_1 - x_1v_2) + b_2(v_2 - v_1) - s_1(x_2v_3 - x_1v_4) - b_1(v_4 - v_3), \\ c_2 &= s_2(v_2 - v_1) - s_1(v_4 - v_3), \quad c_3 = x_1v_2 - x_2v_1 + x_2v_3 - x_1v_4, \\ c_4 &= v_1 - v_2 + v_4 - v_3, \quad c_5 = b_2(x_2v_1 - x_1v_2) - b_1(x_2v_3 - x_1v_4), \\ c_6 &= (s_2 - s_1)(x_2 - x_1), \quad c_7 = (b_2 - b_1)(x_2 - x_1). \end{aligned} \quad (3)$$

The corner velocities v_1, v_2, v_3 and v_4 , are in general, the values linearly interpolated from the specified input values. The coefficients c_1, c_2, \dots, c_7 are pre-calculated for all trapezoids prior to ray tracing.

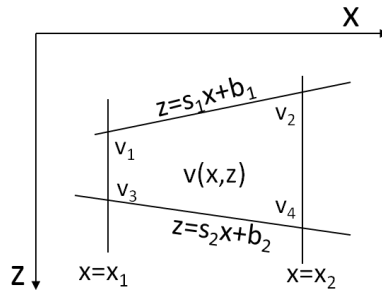


Figure 2: The velocity distribution, $v(x,z)$, inside a model trapezoid is given by (2).

Ray tracing:

Ray tracing through the velocity model is done, using zero-order asymptotic ray theory by solving the ray tracing equations numerically [7]. The ray tracing equations are a pair of first-order ordinary differential equations that can be written in two forms:

$$\frac{dz}{dx} = \cotan \theta, \frac{d\theta}{dx} = \frac{(v_z - v_x \cotan \theta)}{v} \quad \text{or} \quad \frac{dx}{dz} = \tan \theta, \frac{d\theta}{dz} = \frac{(v_z \tan \theta - v_x)}{v} \quad (4)$$

with initial conditions: $x = x_0, \quad z = z_0, \quad \theta = \theta_0$

where θ is the angle between the tangent to the ray and the z axis, v is the wave velocity and v_x and v_z are partial derivatives of velocity with respect to the x and z coordinates. The point (x_0, z_0) is the source location and θ_0 is the ray take-off angle. A Runge-Kutta method [8] based on integration, with error control is used to solve these systems and Snell's law is applied at the intersection of a ray with a layer boundary.

Results

As a result of the experiment, we obtained 6 record sections (Figure 1), allowing the identification of a certain number of crustal and mantle arrivals, and their picking, based on a cross correlation function, with a specified uncertainty.

Travel times obtained are used in addition to the velocity model created as input to run the travel time modeling to produce a geologically meaningful model that minimizes travel time residuals (difference between picked and calculated arrivals)

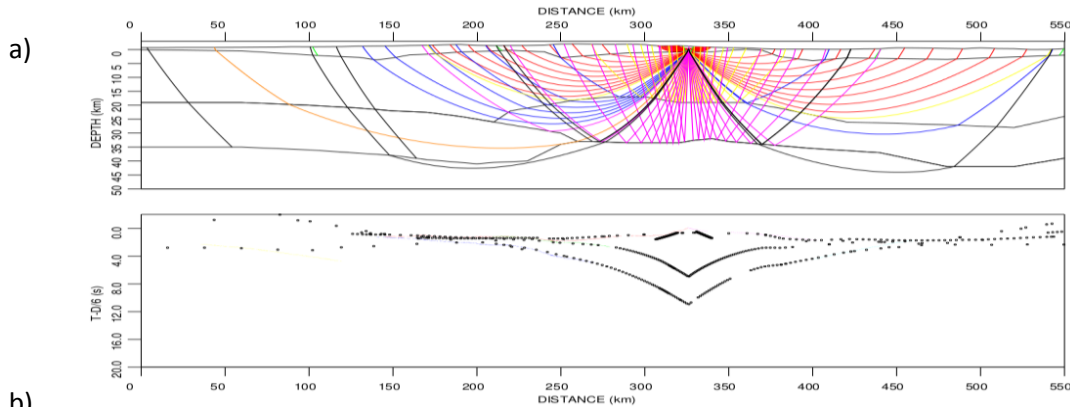


Figure 3: a) Velocity model obtained after forward modeling (raytracing) for shot 1; black lines represent the areas where the boundaries are constrained by incidence rays. b) Calculated (black points) and picked (colored lines) travel times, in reduced time by 6 km/s.

and where rays can be traced for as many picks as possible.

First, the geometry was amended in the velocity model to fit with the data obtained by handheld GPS, and then using the arrival times from the 6 shots, the velocity model was iteratively constructed, to provide a satisfactory match between calculation and observation.

The obtained velocity model is presenting several differences with models obtained from previous studies [1], in particular in the upper part corresponding to the

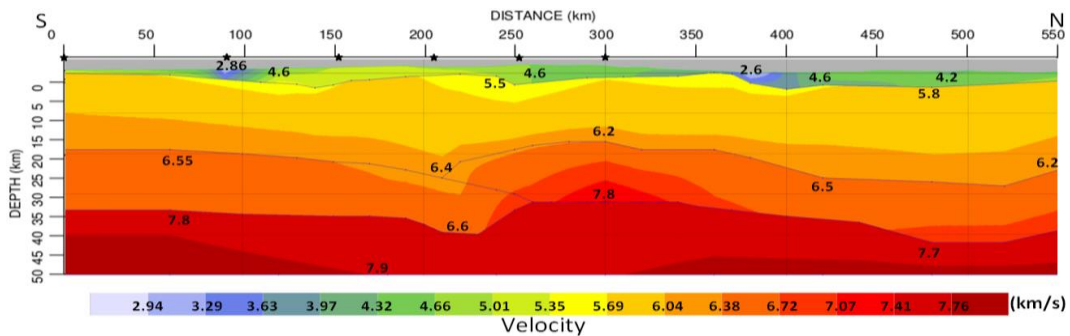


Figure 4: Final velocity model, the values written on the model are the local velocities and the black stars correspond to the shot positions.

sedimentary layer in addition to the shape of the last layer corresponding to the Moho discontinuity.

Conclusion

In this paper, we are suggesting a new solution of the seismic data acquired during the SIMA project, and the velocity model obtained is reflecting the impact of topography in seismic waves propagation.

References

- [1] P. Ayarza, R. Carbonell, A. Teixell, I. Palomeras, D. Marti, A. Kchikach, M. Harnafi, A. Levander, J. Gallart, M.L. Arboleya, J. Alcalde, M. Fernández, M. Charroud, M. Amrhar, Crustal thickness and velocity structure across the Moroccan atlas from long offset wide-angle reflection seismic data: The SIMA experiment, *Geochemistry, Geophysics, Geosystems*, **15** (2014), 1698 - 1717. <http://dx.doi.org/10.1002/2013gc005164>
- [2] F. Ouraini, K. Gueraoui, P. Ayarza, D. Marti, R. Carbonell, M. Harnafi, A. Mridekh, A. Ammar, New numerical and theoretical model to characterize the upper crustal structure of the Moroccan atlas from wide-angle seismic reflection data, *Contemporary Engineering Sciences*, **8** (2015), 279 - 301. <http://dx.doi.org/10.12988/ces.2015.5116>
- [3] C.A. Zelt, R.M. Ellis, Practical and efficient ray tracing in two-dimensional media for rapid traveltimes and amplitude forward modeling, *Canadian Journal of Exploration Geophysics*, **24** (1988), 16 - 31.
- [4] I. Palomeras, R. Carbonell, I. Flecha, F. Simancas, P. Ayarza, J. Matas, D. Martinez Poyatos, A. Azor, F. Gonzalez Lodeiro, A. Pérez-Estaun, Nature of the lithosphere across the Variscan orogen of SW Iberia: Dense wide-angle seismic reflection data, *Journal of Geophysical Research*, **114** (2009), B02302. <http://dx.doi.org/10.1029/2007jb005050>
- [5] C.A. Zelt, R.B. Smith, Seismic traveltimes inversion for 2-D crustal velocity structure, *Geophys. J. Int.*, **108** (2009), 16 - 34. <http://dx.doi.org/10.1111/j.1365-246x.1992.tb00836.x>
- [6] D.P. Shaff, Waveform cross-correlation-based differential travel-time measurements at the Northern Californian seismic network, *Bulletin of Seismological Society of America*, **95** (2005), 2446 - 2461. <http://dx.doi.org/10.1785/0120040221>
- [7] C.A. Zelt, D.A. Forsyth, Modeling wide-angle seismic data for crustal structure: Southeastern Grenville Province, *J. Geophys. Res.*, **99** (1994) 11687-11704. <http://dx.doi.org/10.1029/93jb02764>
- [8] R.E. Sheriff, L. P. Geldart, *Exploration Seismology, 2 ed., Data Processing and Interpretation*, Cambridge University Press, UK, 1995. <http://dx.doi.org/10.1017/cbo9781139168359>

Received: March 18, 2015; Published: July 20, 2015